Sub-nanometer line width and line profile measurement for CD-SEM calibration by using STEM

Kiyoshi Takamasu*[a], Haruki Okitou[a], Satoru Takahashi[a],
Mitsuru Konno[b], Osamu Inoue[b], Hiroki Kawada[b]
[a]The University of Tokyo, Hongo 7-3-1, Bunkyo-ku, Tokyo, JAPAN 113-8656;
[b]Hitachi High-Technologies Corp., Ichige 882, Hitachinaka-shi, Ibaraki-ken, JAPAN 312-8504

ABSTRACT

The novel method of sub-nanometer accuracy (uncertainty) for the line width and line profile measurement using STEM (Scanning Transmission Electron Microscope) images is proposed to calibrate CD-SEM line width measurement. In accordance with the proposed method, the traceability and reference metrology of line width measurements are established using Si lattice structures. First, we define two interfaces of Si-SiO_2 and Si-Air. The interface of Si-SiO_2 is defined as the end of Si lattice structure, and the interface of SiO_2-Air is defined using image intensity of STEM image after metal coating. Second, an image magnification is calculated using 2D Fourier analysis of a STEM image. Third, the edge positions of the line are detected by Si lattice patterns and image intensity. Using the proposed method, the estimated accuracy less than 0.5 nm for the line width of 50 nm is established.

Keywords: line width, line profile, traceability, Si lattice, STEM, CD-SEM, metal coating

1. INTRODUCTION

The line width measurement in semiconductor industry is mainly carried out by CD-SEM (Critical Dimension Scanning Electron Microscope). The sub-nanometer repeatability of the line width measurement can be obtained using CD-SEM[1-3]. However, absolute accuracy of the line width and line profile measurement is not evaluated, and traceability is not established in the measurement[4-6]. The absolute accuracy of the line width and line profile is recently in great demand for physical simulations such as spectrometry and performance evaluations of transistors. The requirements of the reference measuring method for CD-SEM, CD-AFM, OCD (scatterometry) and physical simulations are shown as follows:

- Absolute measurement with sub-nanometer uncertainty,
- Line width and line profile measurement can be carried out, and
- Two interfaces of Si-SiO_2 and SiO_2-Air (outside) can be detected.

Therefore, we started to develop the novel method of the line width and line profile measurement with high absolute accuracy. In this article, the novel method of sub-nanometer accuracy for the line width and line profile measurement using STEM (Scanning Transmission Electron Microscope) images is proposed to establish the reference measuring method for calibrating CD-SEM and CD-AFM line width measurements. In accordance with the proposed method, the traceability of length is established using Si lattice constant and the uncertainty of the line width measurement is evaluated. The targets of the study as follows:

- The definition of the interfaces are clearly defined,
- Novel data processing procedure for STEM image is determined,
- Novel edge detection method is proposed, and
- Traceability is established by the uncertainty estimation on the proposed method.

*takamasu@pe.t.u-tokyo.ac.jp; phone 81 3 5841-6450; fax 81 3 5841-8554; www.nanolab.t.u-tokyo.ac.jp

Metrology, Inspection, and Process Control for Microlithography XXV, edited by Christopher J. Raymond,
Proc. of SPIE Vol. 7971, 797108 · © 2011 SPIE · CCC code: 0277-786X/11/$18 · doi: 10.1117/12.879036

The comparisons between methods with sectional images by STEM or sectional SEM and methods with horizontal images by CD-SEM or CD-AFM are shown in Figure 1. Using the sectional images, interfaces (edge positions) of a line are clearly observed by STEM and sectional SEM. Furthermore, because the Si lattice structure is observed in STEM images, the image magnification is precisely estimated. From these reasons, we select to use STEM in the methods of investigation for the line width[7-10].

Then, the uncertainty of the line width measurement is evaluated with the uncertainty contributors of pixel size, edge detections and repeatability. Using the proposed method, the estimated accuracy less than 0.5 nm for the line width of 45 - 50 nm is established.

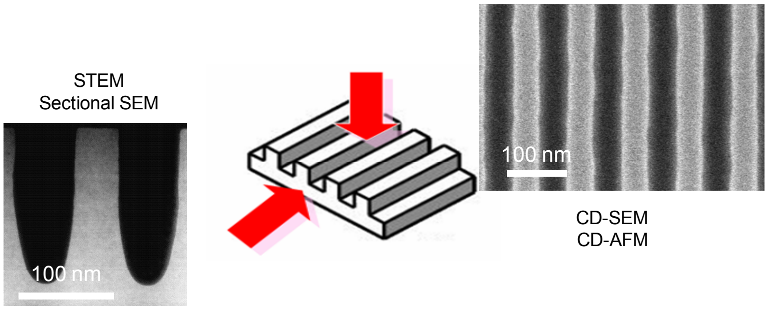

Figure 1. Comparisons between a sectional image by STEM or sectional SEM and a horizontal image by CD-SEM or CD-AFM

2. SAMPLES FOR STEM IMAGES AND DEFINITIONS OF TWO INTERFACES

2.1 Samples for STEM images

Two types STEM images can be obtained as a bright field image by transmission electron and a dark field image by scattered electron shown in Figure 2. The Si lattice structures are clearly observed in these STEM images. Therefore, these types of image are used to define the proposed method in this article.

Figure 3 (a) illustrates a thin specimen of 100 nm thickness in the CD-SEM image. The specimen is a standard of line width of Si wafer, and it is coated by metal and carbon, then it is sliced 100 nm thickness on Si 110 surface by FIB (Focused Ion Beam) micro sampling system[11]. Then the STEM images of the specimen are obtained by STEM[12] (HD-2700) with accelerating voltage of 200 kV and magnification of 70,000 to 3,000,000. Figure 3 (b) shows the example of the specimen in low magnification.

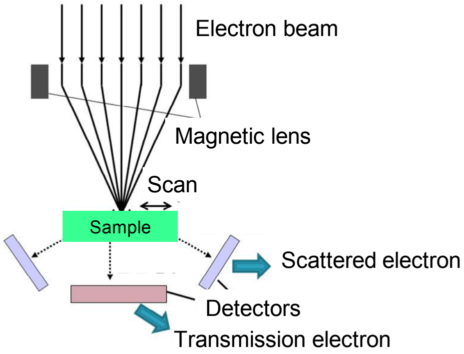

Figure 2. Construction of STEM with two types of detectors for scattered electron and transmission electron.

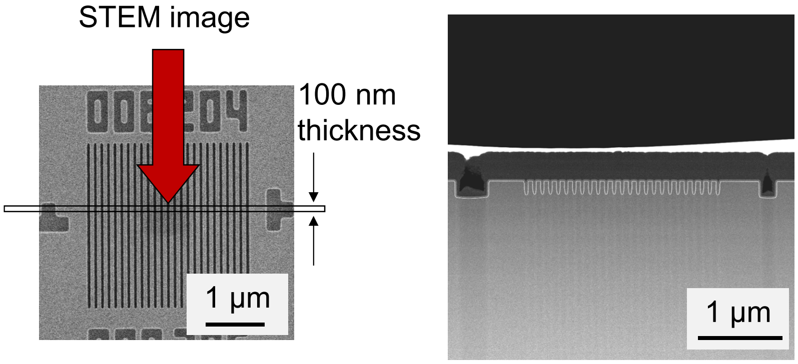

(a) (b)

Figure 3. Sample for STEM image; (a) position of a thin specimen of 100 nm thickness by FIB (Focused Ion Beam) micro sampling system in the CD-SEM image, and (b) STEM image of standard line width of the Si wafer on Si 110 surface in low magnification.

2.2 Definitions for two interfaces of Si-SiO_2 and SiO_2-Air

Figure 4 shows two interfaces of Si-SiO_2 and SiO_2-Air. Si-SiO_2 interface is surface between Si lattice structure and amorphous structure of SiO_2. The Si-SiO_2 interface is detected by emphasizing of Si lattice structure by standard deviation map in the specified frame (see Section 3). And SiO_2-Air interface is surface between SiO_2 and outside of Si line. The SiO_2-Air interface is detected using differences of image intensity between SiO_2 and metal after metal coating on the outside of Si line (see Section 4).

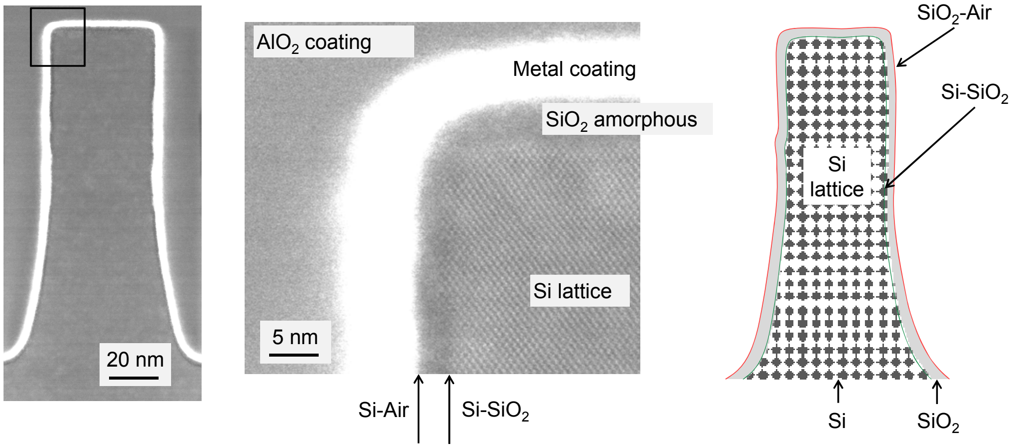

(a) (b) (c)

Figure 4. Si lattice structures and two interfaces (Si-SiO_2 and Si-Air) are observed by a STEM dark field image of the thin spacemen of 100 nm thickness with metal coating; (a) STEM dark field image, (b) Si lattice, SiO_2 amorphous and metal coating in the high magnification image, and (c) model of Si-SiO_2 and SiO_2-Air interfaces.

2.3 Image parameters of STEM image by 2D Fourier analysis

Si lattice structure is observed clearly on the high magnification STEM images. The image parameters as a pixel size and inclination angles of the image are calculated using 2D Fourier analysis. The inside of Si lattice is extracted and transformed to a frequency domain image with zero padding method[15,16]. The positions of peaks of the frequency domain image are compared with the Si lattice pattern, then, an image pixel size and inclination angles of the image are calculated. For instance, the pixel size is calculated as 0.04124 nm/pixel and the inclination angles are calculated as 0.978 arc-degree on X direction and 0.240 arc-degree on Y direction. The inclination angles are mainly caused by drifts during STEM scanning. The variation of pixel size is calculated in four frames at deferent positions of the STEM image. From these calculations, we estimated the standard deviation of magnification is less than 0.15%.

3. EDGE DETECTION OF SI-SIO$_2$ INTERFACE[17]

3.1 Definition of edge for Si-SiO2 interface

Figure 5 (a) shows an example of a bright field STEM image. In the image, Si lattice structure, SiO$_2$ oxide film and Carbon coating can be observed. We define the edge as the end of Si lattice structure for the interface between Si and SiO$_2$. Figure 5 (b) shows the intensity graph on the yellow line of Figure 5 (a), and it indicates that the interface between the Si lattice structure and the oxide film as a red circle.

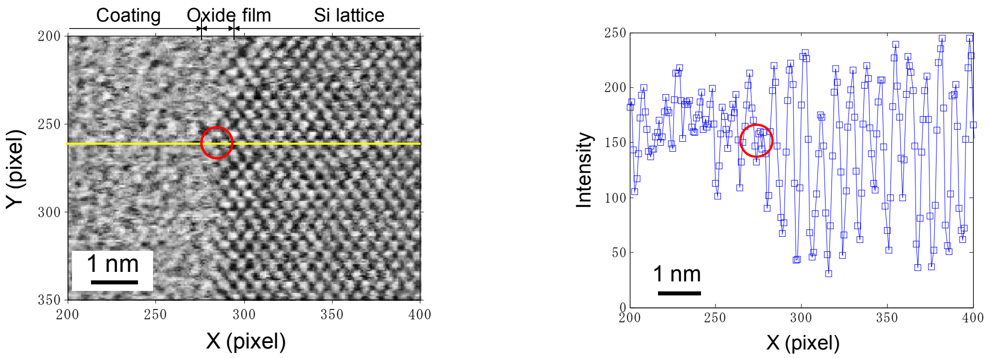

(a) (b)

Figure 5. Definition of the edge (red circle) as the interface of Si lattice structure between Si lattice and SiO$_2$ oxide film; (a) example of a bright field STEM image, and (b) intensity graph on the yellow line.

3.2 Example of edge detection of Si-SiO$_2$ interface

We defined the procedure to detect the edge of Si lattice structure. Figure 6 demonstrates an example of the procedure of the proposed method for the STEM image with accelerating voltage of 200 kV and magnification of 2,800,000 as the follows[17]:

- Original STEM image (Figure 6 (a)),
- Rotated STEM image (Figure 6 (b)),
- Averaging STEM image (Figure 6 (c)),
- Local standard deviation map (Figure 6 (d)),
- Detected edges on the averaging STEM image (Figure 6 (e)), and,
- Detected edges on the rotated STEM image (Figure 6 (f)).

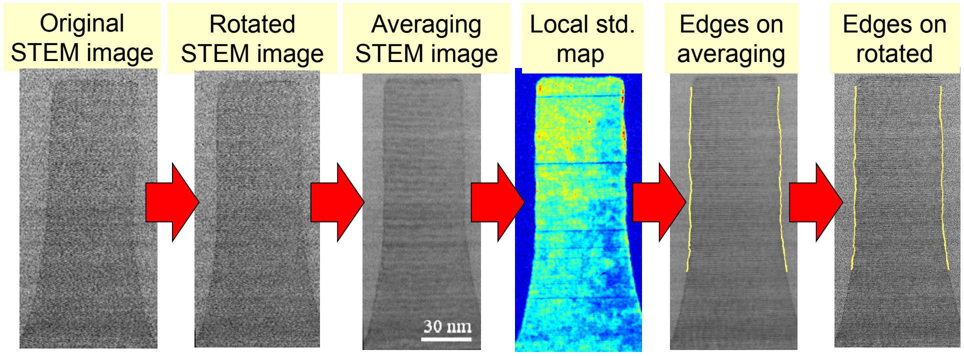

(a) (b) (c) (d) (e) (f)

Figure 6. Example of the procedure of the proposed method[17]; (a) original STEM image, (b) rotated STEM image, (c) averaging STEM image, (d) local standard deviation map, (e) detected edges on the averaging STEM image, and (f) detected edges on the rotated STEM image.

4. EDGE DETECTION OF SIO_2-AIR INTERFACE

4.1 Two types of sample for SiO_2-Air interface

Figure 7 shows two types of metal coating for edge detection of SiO_2-Air interface as follows:

- Type A (Figure 7 (a) and (b)): 23 nm metal coating and 500 µm Carbon coating, and
- Type B (Figure 7 (c) and (d)): 1.5 nm metal coating, 23 nm AlO_2 coating and 500 µm Carbon coating.

After metal coatings, Si line is sliced as the thin sample of 100 nm thickness by FIB (Focused Ion Beam) micro sampling system (FB-2100). Figure 7 (a) shows an example of Type A sample by a dark field STEM image. In the image, Si area (Si lattice structure and SiO_2 oxide film) and metal area (metal coating) can be observed. The thickness of the oxide film varies under circumstance conditions such as atmosphere gas density, temperature, gas pressure, and exposure time for gas. Therefore, we define the edge using metal coating. Figure 8 (b) shows the intensity graph on the black line of Figure 8 (a), and it clearly indicates the interface between the Si area and the metal area by image intensity. Figure 8 (c) and (d) shows a dark field STEM image and image intensity of a Type B sample.

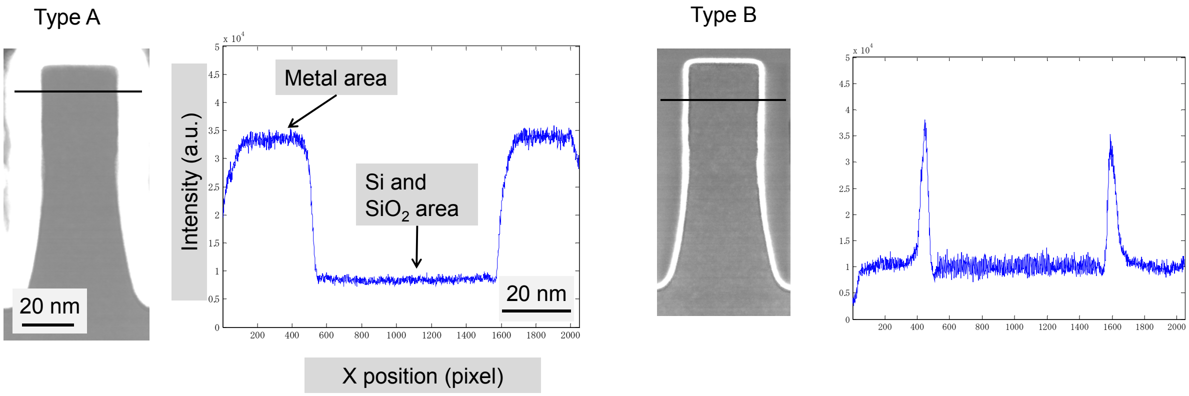

(a) (b) (c) (d)

Figure 7. Definition of the edge as the interface of SiO_2 and outside (Air) between SiO_2 amorphous and metal coating area; (a) example of a dark field STEM image of Si line with metal coating (Type A), (b) intensity graph on the black line of (a), (c) example of a dark field STEM image of Si line with metal and AlO_2 coating (Type B), (d) intensity graph on the black line of (c).

4.2 Definition of edge and data processing method for SiO_2-Air interface

Figure 8 (a) shows the image intensity graph of a Type A sample. The value of intensity clearly indicates the interface between Si area and metal area, and then the position of 50% of the intensity value is defined as SiO_2-Air interface. The standard deviation in each area is 3% in metal coating area and 6% in Si area, then after averaging in metal coating and Si area, 50% threshold level is varied in less than ±1%. Figure 8 (b) illustrates the intensity graph for the part of Si line.

Figure 9 shows the data processing of edge detection from image intensity graph. First, average values in the metal area and the Si area are calculated, and then 50% threshold level and left and right positions of the edges are detected. Error of edge positions are estimated from ±1% variation of threshold level. For instance, 50% intensity level is 20908 (at Y position is 500 pixel) and the slope in 50% is 420/pixel in Figure 9, the threshold level of ±1% variation causes the variation of edge position less than ±0.05 nm.

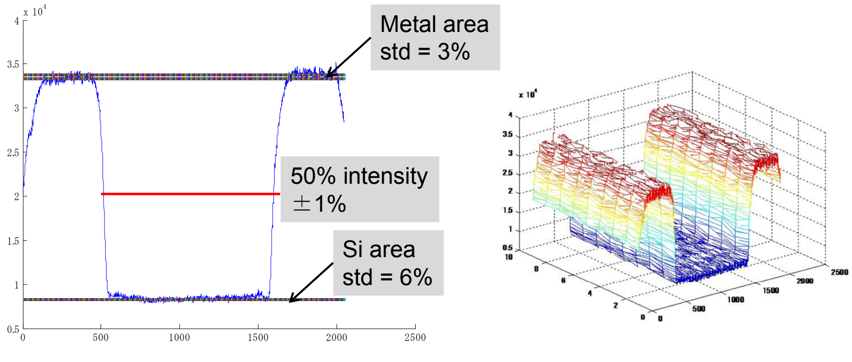

(a) (b)

Figure 8. Image intensity graph of a Type A sample; (a) example of image intensity, and (b) intensity graph for the part of Si line.

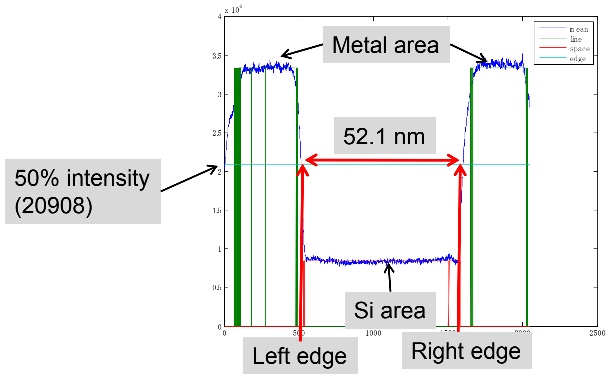

Figure 9. Data processing from the image intensity graph of a Type A sample. Average values in metal area and Si area are calculated, then 50% threshold level and left and right edges detected.

4.3 Example of edge detection for SiO2-Air interface

We defined the procedure to detect SiO_2-Air interface on sections 4.1 and 4.2. Figure 10 demonstrates an example of the procedure of the proposed method for the Type A sample. The size of image pixel is defined as 0.048 nm/pixel by the nominal magnification of STEM image. Line width 48.7 nm - 52.3 nm on 21.6 nm area is calculated in Table 1.

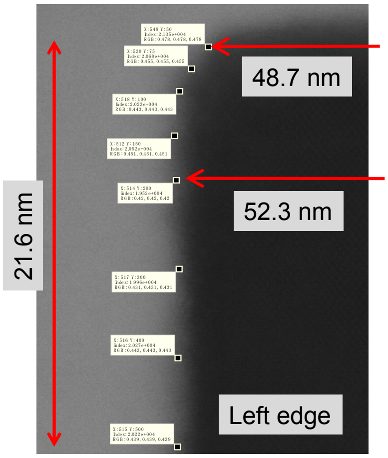

Figure 10. Example of the edge detection and line width calculation. Line width of 48.7 nm - 52.3 nm on 21.6 nm area is calculated.

Table 1. Example of edge detection for SiO_2-Air interface. Left and right edges are detected and line width is calculated by the size of image pixel defined as 0.048 nm/pixel by the nominal magnification of STEM image.

Y position (pixel)	**Left edge position (pixel)**	**Right edge position (pixel)**	**Line width (pixel)**	**Line width (nm)**
50	548	1562	1014	48.7
75	530	1584	1054	50.6
100	518	1593	1075	51.6
150	512	1602	1090	52.3
200	514	1601	1087	52.2
300	517	1599	1082	51.9
400	516	1598	1082	51.9
500	515	1601	1086	52.1

5. CONCLUSIONS AND FUTURE WORKS

The novel method of sub-nanometer accuracy for the line width and line profile measurement using STEM images is proposed to calibrate of CD-SEM line width measurement. In the proposed method, the traceability and reference metrology of line width standards are established using Si lattice structures. Using STEM images, the line width is calculated the following procedure:

- We define two types of interface of Si-SiO_2 and SiO_2-Air.
- The specimen is coated by metal and carbon, then, it is sliced 100 nm thickness on Si 110 surface by FIB (Focused Ion Beam) micro sampling system.
- STEM images of the specimen are obtained by STEM (HD-2700).
- The image magnification (pixel size) and inclination angles of the STEM image are calculated by the peeks of the frequency domain image using 2D Fourier analysis.
- The edge positions of Si-SiO_2 interface are detected at the 50% intensity of the local standard deviation map of the STEM image.
- The edge positions of SiO_2-Air interface are detected at the 50% intensity of the image intensity graph of STEM image after metal coating.

The proposed method was applied to an example of Si line specimen, and the line width is calculated with the estimated accuracy less than 0.5 nm. In future works, we will compare the line width by STEM images using the proposed method and the results by CD-SEM images and CD-AFM images on the same line positions. Then the detailed estimation of the uncertainty of the proposed method is calculated for establishment of the traceability.

REFERENCES

1. Nakayama, Y., Gonda, S., Misumi, I., Kurosawa, T., Kitta, J. Mine, H., Sasada, K., Yoneda, S. and Mizuno, T., "Novel CD-SEM calibration reference patterned by EB cell projection lithography," Proc. SPIE 5752, 591-602 (2005).
2. Yamaguchi, A., Fukuda, H., Kawada, H. and Iizumi, T., "Impact of long-edge roughness (LER) on accuracy in critical dimension measurement and new guideline for CD metrology," Jpn. J. Appl. Phys. 44, 5575-5580 (2005).
3. Villarrubia, J. S., Vladar, A. E. and Postek, M. T., "A simulation study of repeatability and bias in the CD-SEM," Proc. SPIE 5038, 138-149 (2003).
4. Nakayama, Y., Kawada, H., Yoneda, S. and Mizuno, T., "Novel CD-SEM calibration reference consisting of 100-nm pitch grating and positional identification mark," Proc. SPIE 6518, 65183J (2007).

5. Abe, H., Hamaguchi, A. and Yamazaki, Y., "Evaluation of CD-SEM measurement uncertainty using secondary electron simulation with charging effect," Proc. SPIE 6518, 65180L (2007).
6. Dixson, R. and Orji, N. G., "Comparison and uncertainties of standards for critical dimension atomic force microscope tip width calibration," Proc. SPIE 6518, 651816 (2007).
7. Hasler-Grohne, W., Frase, C. G., Czerkas, S., Dirscherl, K., Bodermann, B., Mirande, W., Ehret, G., and Bosse, H., "Calibration procedures and application of the PTB photomask CD standard," Proc. SPIE 5992, 59924O (2005).
8. Bosse, H., Mirande, W. and Frase, C. G., "Comparison of linewidth measurements on COG masks," Proc. SPIE 4349, 99-108 (2001).
9. Lowney, J. R., "Use of Monte Carlo modeling for interpreting scanning electron microscope linewidth measurements," Scanning 17, 281-286 (1995).
10. Liu, H.-C., Fong, D., Dahlen, G. A., Osborn, M., Hand, S. and Osborne, J. R., "Carbon nanotube AFM probes form microlithography process control," Proc. SPIE 6152, 61522Y (2006).
11. http://www.hitachi-hitec.com/global/em/fib/fib_index.html
12. http://www.hitachi-hitec.com/global/em/tem/tem_index.html
13. http://physics.nist.gov/cgi-bin/cuu/Value?asil
14. Barth, J. V., Costantini, G. and Kern, K., "Engineering atomic and molecular nanostructures at surfaces," Nature 437, 671-679 (2005).
15. Larkin, K. G., Oldfieldb, M. A. and Klemma, H., "Fast Fourier method for the accurate rotation of sampled images", Optics Communications 139, 99-106 (1997).
16. Brigham, E. O., "The fast Fourier transform and its applications," Prentice-Hall, Englewood Cliffs, NJ, (1988).
17. Takamasu, K., Kuwabara, K., Takahashi, S., Mizuno, T., Kawada, H., "Sub-nanometer Calibration of CD-SEM Line Width by Using STEM," Proc. SPIE 7638 - 55 (2010).